Automatic Segmentation Algorithm of Solar Cells Based on Grid Corner Extraction

1st Xinyi Chen
The Key Laboratory of Measurement and Control of CSE, Ministry of Education
College of Automation
Southeast University
Nanjing, China
xinyichen98@163.com

2nd Kanjian Zhang
Southeast University Shenzhen Research Institute
Shenzhen, China
The Key Laboratory of Measurement and Control of CSE, Ministry of Education
College of Automation
Southeast University
Nanjing, China
kjzhang@seu.edu.cn

3nd Jinxia Zhang*
Southeast University Shenzhen Research Institute
Shenzhen, China
The Key Laboratory of Measurement and Control of CSE, Ministry of Education
College of Automation
Southeast University
Nanjing, China
jinxiazhang@seu.edu.cn

***Abstract*—Defect detection in photovoltaic (PV) panels based on electroluminescence (EL) images has been a prominent approach in the field. These approaches rely on pre-segmented PV cells as input. However, practical EL images suffer from background interference and image deformation caused by variations in perspective, making the segmentation and extraction of PV panel cells challenging. To overcome these issues, algorithm ASSC(Automatic Segmentation of Solar Cells) is proposed. Concretely, a combination of Image processing techniques and convolutional network is employed to address these problem. Additionally, image deformation is tackled by implementing perspective correction, which transforms the PV panel into a front view. Moreover, the semantic segmentation network is leveraged to extract the grid corner points of PV panels. Compared to traditional image techniques, ASSC offers a more accurate solution without prior knowledge of PV panel specifications. Experimental results on a dataset collected on site demonstrate the effectiveness of ASSC which achieves an IoU(Intersection over Union) metric of up to 97.25%.**

***Index Terms*—Automatic segmentation, Grid corner extraction, Photovoltaic(PV) modules, Electroluminescence image, Deep learning**

I. Introduction

Facing the challenges of renewable energy and environmental pollution, solar energy has been widely developed and utilized as an important clean energy source. Photovoltaic (PV) panels, as the core components of solar power generation, have seen increasing production year by year. However, defects such as scratches, damages, hotspots, stains, and grid interruptions inevitably occur on the surface of PV panels, both during industrial production and usage [1]. These defects can negatively impact the conversion efficiency and safety of PV panels [2], thus affecting the overall stability of PV power generation. Therefore, fault detection of PV cells holds significant practical significance.

Because of the easy access of electroluminescence (EL) images, defect detection based on EL images is the mainstream method in the field of surface defect detection of solar cells. In the early years, traditional image processing techniques were employed for defect detection in EL images. Studies [3], [4] primarily employed bitwise OR methods for enhancing EL images. Tsai et al. [5] proposed an independent component analysis technique. Su et al. [6] proposed center pixel gradient information to center-symmetric local binary pattern to obtain more identifiable defect features in the presence of non-uniform background interference.

With the popularity of deep learning, defect detection based on deep learning has become a research hot spot in this field. Bartler et al. [7] proposed an improved classification network based on the VGG16 [8] architecture and investigated the impact of minority oversampling and data augmentation on performance improvement. Deitsch et al. [9] employed the VGG19 network and SVM to propose two crack classification methods. Su et al. [10] improved the region proposal network (RPN) based on Faster R-CNN [11] for detecting small cracks in PV modules. Inspired by the VGG11 network, Akram et al. [12] designed a 9-layer convolutional network structure and validated it on the ELPV public dataset.

However, these methods rely on pre-segmented PV panel cells for detection, which significantly deviates from the actual input images in real industrial environments. In practical industrial scenarios, PV panels exhibit diverse appearances in EL images due to variations in specifications and different material processes. This poses considerable challenges for the automatic segmentation of PV panel cells. Currently, there is limited research focusing on automatic segmentation tasks for PV panel cells, with most methods [13]–[15] relying on manually designed features combined with thresholding based on pixel distribution in the images. But external factors such as background noise and lighting conditions significantly impact pixel values, making the selection of thresholds crucial for segmentation effectiveness. This misalignment with the concept of automatic segmentation highlights the existing gap in this area of research.

The automatic segmentation algorithm of PV panel cells based on grid corner detection is proposed for this. Specifically, preprocessing techniques such as image denoising, binarization, and coordinate transformation is firstly applied to convert the input images into images in a front view. Subsequently, the four corner points of each PV panel cell are detected and these detected corner points are utilized to accurately locate each PV panel cell. For those corner points that are not detected, a complementary approach based on the overall distribution of corner points is employed to fill in the missing information, thereby achieving precise segmentation of each PV panel cell. As we know, we are the first to propose the adoption of a grid corner point detection approach for PV panel cell segmentation. Compared to studies that employ traditional object detection methods for this task, proposed ASSC(Automatic Segmentation of Solar Cells) offers lower annotation costs and achieves superior segmentation results.

The main contributions of this paper are as follows:

- We propose ASSC for the automatic segmentation of PV panel cells based on grid corner point extraction, which overcomes the reliance on thresholding and enhances the robustness of the algorithm.
- Experimental results on a field collected dataset demonstrate the effectiveness of ASSC.
- ASSC is poised to become a novel research paradigm in the field of PV panel cell segmentation.

II. Related Work

Currently, there are few algorithms for segment PV cell images from EL images. Most studies currently rely on traditional image processing methods. Liu et al. [13] utilized the minimum bounding rectangle algorithm to extract the main areas of PV panels and segments PV cells based on the row and column pixel distributions of binary Sobel edge images. Pratt et al. [14] also employed pixel distribution to segment PV panel cells. Tang et al. [15] adopted line detection to identify cell layouts. There are also studies that leverage deep learning to achieve automatic segmentation of PV panel cells. For instance, Otamend et al. [16] utilized Faster R-CNN to detect the bounding boxes of PV panel cells and perform segmentation. However, this approach involves high annotation costs and requires a substantial amount of data.

There are also several studies focusing on the segmentation of PV panel cells from images captured by unmanned aerial vehicles (UAVs). Vega et al. [17] proposed two extraction methods based on traditional image processing techniques and deep learning. In contrast to EL images, images captured by UAVs are often taken from higher viewpoints, resulting in increased background interference and the presence of multiple PV panels within a single image. Consequently, some studies focus on correcting camera lens distortion. For instance, Deitsch et al. [9] established a lens distortion model to rectify distortion phenomena such as curved lines. However, in EL images, each image typically contains a single PV panel captured at a moderate distance nd does not exhibit lens-induced distortion such as curved lines. Therefore, research based on UAV-captured images has limited relevance and applicability to EL image analysis. Due to the presence of more background interference in UAV-captured images and the higher difficulty of recognizing numerous PV panels in a single image, these methods are more complex than the former ones.

III. Method

A. Model Overview

To achieve rapid and accurate extraction of PV panel cells, ASSC employs traditional image processing techniques to preprocess EL images, combined with a deep learning algorithm to extract the corner points of each PV panel cell. Based on the above process, ASSC is proposed for PV panel cells based on grid corner detection. ASSC combines the advantages of traditional image processing and deep learning methods, presenting a PV cell segmentation and extraction algorithm based on grid corner point extraction from EL images. This method can start from images without the need for large amounts of data and does not rely on the specifications of PV panels.

The appearance of PV modules in EL images is influenced by various factors, making automatic segmentation and extraction of PV cell images challenging. The specifications and different material processes of PV panels result in variations in the spacing and layout of solar cells in EL images. Additionally, busbars and some defective areas of solar cells can be mistakenly identified as cell boundaries. Therefore, in practical applications, it is necessary to use computer vision techniques with strong feature expression ability to accomplish the task of segmenting PV panel cells. Another drawback of traditional image algorithms is the need for threshold adjustments when dealing with images from different data sources. Background noise and lighting conditions greatly affect pixel values, which can interfere with grid point segmentation tasks. To reduce the requirement for manual threshold adjustment, ASSC uses a segmentation algorithm for adaptively extracting the corner points of the grid. Furthermore, considering that each EL image of an on-site captured PV panel contains relatively clean background and is captured at an appropriate distance without lens-induced line curvature distortion, ASSC aims to achieve both speed and accuracy by the method proposed.

Fig. 1 illustrates the complete workflow of ASSC. ASSC comprises two parts: perspective correction and grid corner extraction. The first step makes the background in the image completely eliminated and convert PV panels image into a front view. In the second step, a lightweight model is employed to capture the grid corner points. Ultimately, by determining the position of the grid based on the distribution of corner points, ASSC achieves precise segmentation of each PV panel cell.

B. Perspective Correction

As illustrated in the input part of Fig. 1, the original EL images exhibit two issues:

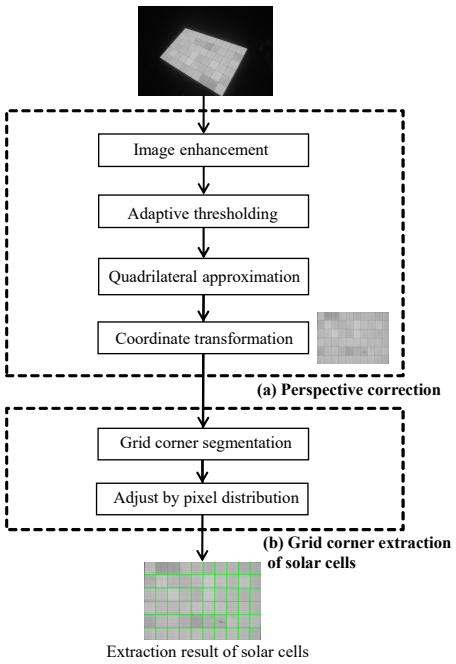

Fig. 1: Overall workflow of ASSC(Automatic Segmentation of Solar Cells).

1. The presence of a considerable amount of black background surrounding the solar cell modules.

2. Variation in the shape of the PV panels due to differences in capturing angles.

These two problems hinder the direct utilization of EL images as inputs for the segmentation model. To address the background issue, histogram normalization and contrast enhancement techniques are initially employed to enhance the contour of the PV panels. Subsequently, adaptive thresholding is employed to separate the PV panels from the background in the EL images. Regarding the issue of PV panel deformation, leveraging the prior knowledge that PV panels possess a rectangular shape, quadrilateral detection is employed to obtain the coordinates of the four corner points. By incorporating perspective transformation, ASSC rectifies the PV panels to a normal view, thus mitigating the effect of shape deformation.

1) Quadrilateral Approximation: Based on the analysis of the original EL images, it is observed that the background of most images is close to black, while the solar cell area generally exhibits distinct grayscale differences from the background. As a result, the histograms of most images have two peaks or exhibit a bimodal distribution. This implies that if a threshold value can be set to the middle value between the two peaks, it is possible to separate the two regions. Considering that the grayscale peak values may not be exactly the same in different images, the Otsu thresholding algorithm [18] is used. The Otsu algorithm is a classic image binarization algorithm that can adaptively differentiate the foreground and background regions based on the pixel value distribution across the entire image, thus distinguishing the battery and non-battery areas in EL images. To enhance the overall contour of the PV panels, a closing operation is also employed to bridge any potential gaps that may occur in between. After the aforementioned operations, the interference caused by the background is largely eliminated. As a result, the contour of the largest connected component in the image can be considered as the contour of the PV panel.

To obtain the coordinates of the four corner points, the binary images are subjected to quadrilateral contour approximation [19]. The principle involves first extracting the contour point set based on the canny algorithm and then performing calculations and approximations on the obtained contour point set. The process begins by identifying the two points that are farthest apart in the contour point set and connecting them. Then, on the contour, a point that is farthest from the current line is found, and this point is connected to the existing line to form a closed polygon, resulting in a triangle. This iteration continues until all points on the contour are within a small constant distance from the current polygon. At this point, the coordinates of the approximated quadrilateral's corner points are obtained.

2) Coordinate Transformation: Once the coordinates are obtained, the perspective images can be transformed into images captured under a normal view. Perspective transformation can correct distortions caused by the camera not being parallel to the capture plane and obtain the orthographic projection of the object [15]. In this case, the obtained four-corner points are directly transformed into the four corner points of the corrected image. The perspective transformation model is shown in (1):

$$\begin{bmatrix} x \\ y \\ z \end{bmatrix} = \begin{bmatrix} a_{11} & a_{12} & a_{13} \\ a_{21} & a_{22} & a_{23} \\ a_{31} & a_{32} & 1 \end{bmatrix} \begin{bmatrix} u \\ v \\ 1 \end{bmatrix}. \tag{1}$$

The normalized coordinates of the corner points are:

$$\begin{bmatrix} x' \\ y' \\ z' \end{bmatrix} = \begin{bmatrix} \frac{x}{z} \\ \frac{y}{z} \\ \frac{z}{z} \end{bmatrix} = \begin{bmatrix} \frac{a_{11}u+a_{12}v+a_{13}}{a_{31}u+a_{32}v+1} \\ \frac{a_{21}u+a_{22}v+a_{23}}{a_{31}u+a_{32}v+1} \\ 1 \end{bmatrix}. \tag{2}$$

To calculate the eight unknown variables, ASSC only needs four pairs of point coordinates to obtain the transformation matrix.

C. Grid Corner Extraction of Solar Cells

After perspective correction, the PV panel image is fixed in the plane coordinate system, which facilitates the subsequent extraction of individual solar cells. Considering that the gaps between most solar cells appear as black boundaries but the cracks in the solar cells also have dark colors, relying solely on pixel distribution in rows and columns may lead to errors in the results. To adapt to the task of extracting solar cells without prior knowledge of the number of rows and columns, semantic segmentation model is employed to extract the corner points. This further allows for the extraction of individual cell images by dividing the solar cells. Since the grid corner points of solar cells from different specifications have similar characteristics, learning the features of grid corner points brings better robustness and adaptability to the extraction process.

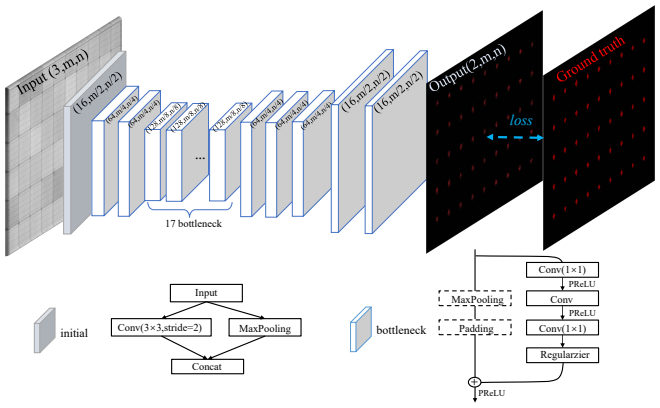

Fig. 2: Network structure of grid corner segmentation model.

1) Semantic Segmentation Model to Extract Corner Points: The lightweight segmentation network ENet [20] is employed for corner point segmentation in this step. ENet employs parallel pooling and convolution operations in the initial block, which effectively accelerates the inference speed during the network's execution. Additionally, the network applies feature map compression, as well as asymmetric convolution and dilated convolution, to reduce computational complexity. Considering that the semantic information in solar panel images is less complex compared to other scenes, compressing the features redundantly is acceptable and also beneficial for fast deployment in practical scenarios. The segmentation model of grid corner points is illustrated as Fig.2 shown. The cross entropy loss is used as the loss function.

2) Grid Conner Adjustment by Pixel Distribution: After obtaining the segmentation results, further processing is required to determine the coordinates of each corner point. This process involves considering the regions in the segmentation results and addressing cases where certain corner points are not segmented. To achieve this, pixel distribution information is incorporated as a comprehensive approach to handle missing or redundant points.

To analyze the distribution of grayscale values, the predicted image is reversed in rows and columns, and the grayscale distribution is computed. The resulting grayscale distribution waveform reveals that each peak represents a gap between solar cells. Due to the regular arrangement of PV cells, these valleys also exhibit relatively equidistant distribution. While the number and distribution of cells may vary across different solar panels, most gaps should be relatively consistent. Noise interference can be mitigated by comparing the grayscale values with the mean value of the gaps. Finally, the centroid coordinates of each point set is selected as the final row and column positions.

IV. Experimental Results

A. Dataset

The experiment is based on 92 original EL images taken at the Cha'an Temple and Louzi Village Photovoltaic Power Station in Badong, HuBei province. These images contain PV panel images with four different specifications, including a 6×24 specification(6 rows, 24 columns), a 6×12 specification, and two variations of a 6×10 specification.

In this study, the dataset is divided according to a ratio of 75% and 25%, with 23 images used as a test set for evaluating the model's performance in subsequent steps. The train set is used to train the grid corner segmentation network. Considering the different distributions of the dataset specifications, the dataset is divided proportionally as shown in Table. I.

Due to the variable size of the original image, the length and width of the image are both more than thousand pixels, and the length and width of the corrected front view image are also too large. In order to facilitate network computation and meet computing power requirements, the input image of the semantic segmentation network will be scaled to a size of 600 × 400. The optimizer used is the Adam optimizer with default parameters. The training of the semantic segmentation network for extracting grid corner points is performed using one GPU GeForce RTX 3090 with 60 epochs.

B. Evaluatation metrics

Considering the need for quantitative assessment of PV panel cell extraction accuracy, intersection over union (IoU) is utilized to measure the overlap between the original and predicted positions of each PV panel cell. IoU can measure the overlap between prediction position and true position by comparing the intersection and union. Since the original annotations are based on the regions around the corner points of each grid, the center coordinates of each annotation region are computed first by calculating the centroids of connected components. This allows for the calculation of metrics based on the four corner point coordinates of each PV panel cell.

IoU [21] is a crucial concept in object detection, representing the intersection over union ratio between the predicted bounding box and the ground truth bounding box. It measures the overlap between these two boxes by comparing their intersection and union. An IoU value of 1 indicates a perfect overlap. In this study, IoU is used to evaluate the accuracy of PV panel cell extraction.

The bounding box of a PV panel cell can be represented by the coordinates of its top-left and bottom-right corners. Assume that there are two PV panel cells: A : $((x_{a_1}, y_{a_1}, x_{a_2}, y_{a_2}))$ and B : $(x_{b_1}, y_{b_1}, x_{b_2}, y_{b_2})$. The coordinates of their overlapping region C can be represented as

TABLE I: Dataset division

Dataset	Type 1 (6row,24col[a])	Type 2 (6row,12col)	Type 3 (6row,10col)	Type 4 (6row,10col)	$\sum$
Train	24	22	19	4	69
Test	8	7	6	2	23
					92

[a]It means the PV panel has a 6-row by 24-column specification.

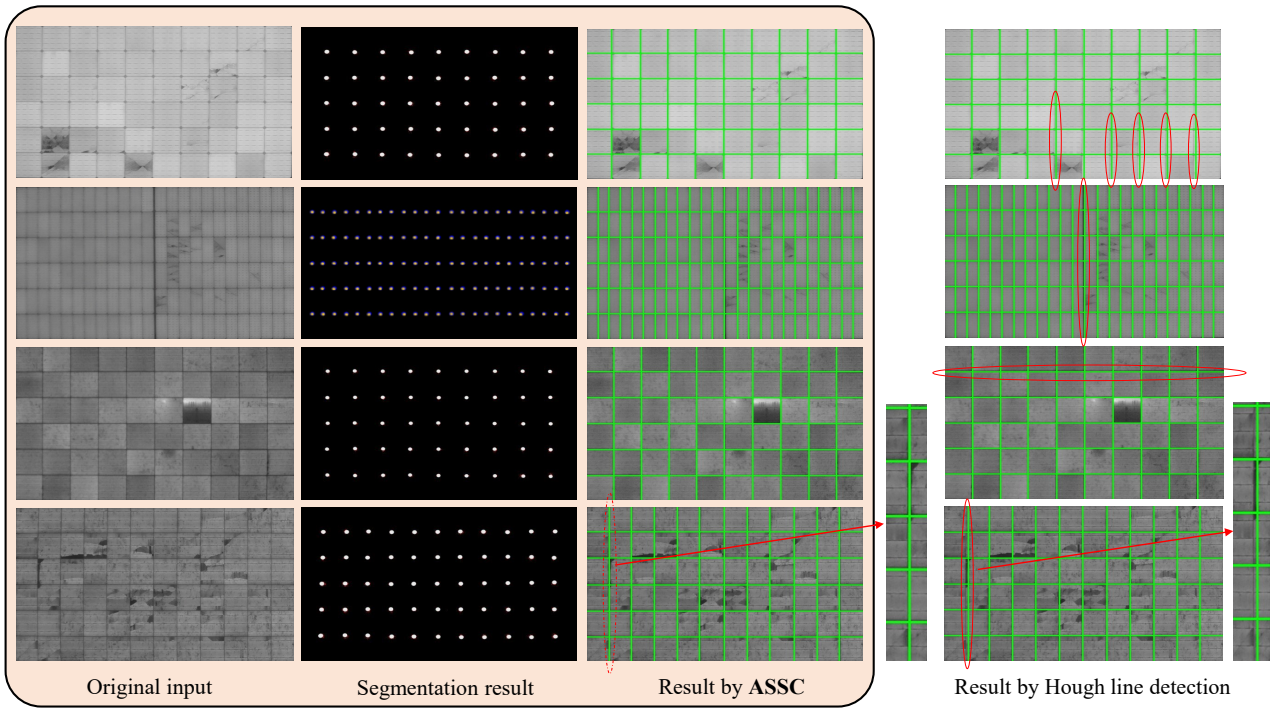

Fig. 3: Visual segmentation results of ASSC and detail comparison.

$(x_{c_1}, y_{c_1}, x_{c_2}, y_{c_2})$ as in (3):

$$\begin{bmatrix} x_{c_1} \\ y_{c_1} \\ x_{c_2} \\ y_{c_2} \end{bmatrix} = \begin{bmatrix} \max(x_{a_1}, x_{b_1}) \\ \max(y_{a_1}, y_{b_1}) \\ \min(x_{a_2}, x_{b_2}) \\ \min(y_{a_2}, y_{b_2}) \end{bmatrix}. \tag{3}$$

According to (4), the overlapping area value is obtained:

$$intersection = \max(x_{c_2} - x_{c_1} + 1.0, 0) \cdot \max(y_{c_2} - y_{c_1} + 1.0, 0). \tag{4}$$

The union of the two boxes is determined by (5) and (6), where (6) represents the calculation of the areas of the two boxes.

$$union = S_A + S_B - intersection, \tag{5}$$

$$\begin{cases} S_A = (x_{a_2} - x_{a_1} + 1.0) \cdot (y_{a_2} - y_{a_1} + 1.0). \\ S_B = (x_{b_2} - x_{b_1} + 1.0) \cdot (y_{b_2} - y_{b_1} + 1.0). \end{cases} \tag{6}$$

The final formula for calculating the IoU is as follows:

$$IoU = \frac{intersection}{union}. \tag{7}$$

C. Qualitative and Quantitative Evaluation

In this section, the extraction performance of PV panel cells are analysed from two aspects: visualization results and IoU. To compare the effectiveness of ASSC, the performance of a classical algorithm based on Hough line detection [22] are also displayed as a comparison. After binarizing and performing edge detection on the images, Hough line detection is then used to calculate the row and column positions. It is worth noting that this method requires prior knowledge of the number of rows and columns because it needs extra thresholding to filter out computed lines.

Different sets of test images of various specifications are presented as shown in Fig. 3. The second column shows the corner positions after semantic segmentation network and pixel distribution adjustment. The third column demonstrates the visual effects of ASSC, which can effectively divide the PV panel cells. The fourth column shows the results obtained using Hough line detection, and it can be observed that compared to ASSC, there are certain deviations in the division of some rows and columns in the fourth column, especially in the last image.

To quantitatively compare the effectiveness of the methods, IoU is calculated for each PV panel cell using (7) and the average value is taken as the metric, as shown in Table. II. It can be seen that ASSC achieves an IoU value of 97.25%, whereas the algorithm solely based on Hough line detection achieves only 83.11%. This demonstrates the effectiveness of ASSC in the PV panel cell extraction task.

The IoU on images of different specifications are calculated

TABLE II: IoU performance of the automatic segmentation algorithm on the test set of PV cell images

Method	IoU
Hough line detection	0.8311
ASSC	**0.9725**

TABLE III: IoU performance of the automatic segmentation algorithm on each type of the test set of PV cell images

Method	Type 1 (6row,24col[a])	Type 2 (6row,12col)	Type 3 (6row,10col)	Type 4 (6row,10col)
Hough line detection	0.7924	0.8743	0.8835	0.8753
ASSC	**0.9802**	**0.9649**	**0.9209**	**0.9844**

[a]It means the PV panel has a 6-row by 24-column specification.

separately, as shown in Table. III. It can be observed that ASSC achieves high accuracy on various types of PV panel images and significantly outperforms traditional methods.

Although classical methods like Hough line detection can achieve certain results, traditional methods rely too heavily on pixel information, thresholding, or manual filtering. They often require prior knowledge of the number of rows and columns, whereas ASSC does not require prior information about the number of PV panel specifications. Instead, it extracts the corner positions, calculates the row and column numbers using the corner information, and learns the corner features through the segmentation network. Compared to traditional methods, ASSC is less susceptible to interference from background noise in the images.

V. Conclusion

For the task of segmenting PV panel cells, it is the first to propose the adoption of a grid corner point extraction approach. Compared to previous methods, this novel algorithm reduces the reliance on thresholding and exhibits better adaptability to backgrounds and noise. To address the challenges posed by background interference and varying perspectives in the original EL images, perspective correction techniques is employed to transform them into images of a front view. Based on the perspective corrected EL images, semantic segmentation network is utilized to detect the grid corner points of PV panel cells. To mitigate the risk of missing corner points, the proposed method incorporate an automatic fitting approach based on the overall distribution of corner points. By adopting corner point segmentation instead of direct object detection, the method can effectively reduce the dependence on annotated data. Experimental results have demonstrated the effectiveness of ASSC and it can achieve an IoU metric of up to 97.25%. In future this research may provides a new perspective in the field of automatic PV panel cell segmentation.

References

[1] S. W. Ko, Y. C. Ju, H. M. Hwang, J. H. So, Y.-S. Jung, H.-J. Song, H.-e. Song, S.-H. Kim, and G. H. Kang, "Electric and thermal characteristics of photovoltaic modules under partial shading and with a damaged bypass diode," *Energy*, vol. 128, pp. 232–243, 2017.

[2] M. Dhimish, V. Holmes, B. Mehrdadi, and M. Dales, "The impact of cracks on photovoltaic power performance," *Journal of Science: Advanced Materials and Devices*, vol. 2, no. 2, pp. 199–209, 2017.

[3] M. Dhimish, V. Holmes, and P. Mather, "Novel photovoltaic micro crack detection technique," *IEEE Transactions on Device and Materials Reliability*, vol. 19, no. 2, pp. 304–312, 2019.

[4] M. Dhimish and V. Holmes, "Solar cells micro crack detection technique using state-of-the-art electroluminescence imaging," *Journal of Science: Advanced Materials and Devices*, vol. 4, no. 4, pp. 499–508, 2019.

[5] D.-M. Tsai, S.-C. Wu, and W.-Y. Chiu, "Defect detection in solar modules using ica basis images," *IEEE Transactions on Industrial Informatics*, vol. 9, no. 1, pp. 122–131, 2012.

[6] B. Su, H. Chen, Y. Zhu, W. Liu, and K. Liu, "Classification of manufacturing defects in multicrystalline solar cells with novel feature descriptor," *IEEE Transactions on Instrumentation and Measurement*, vol. 68, no. 12, pp. 4675–4688, 2019.

[7] A. Bartler, L. Mauch, B. Yang, M. Reuter, and L. Stoicescu, "Automated detection of solar cell defects with deep learning," in *2018 26th European signal processing conference (EUSIPCO)*, pp. 2035–2039, IEEE, 2018.

[8] K. Simonyan and A. Zisserman, "Very deep convolutional networks for large-scale image recognition," *arXiv preprint arXiv:1409.1556*, 2014.

[9] S. Deitsch, V. Christlein, S. Berger, C. Buerhop-Lutz, A. Maier, F. Gallwitz, and C. Riess, "Automatic classification of defective photovoltaic module cells in electroluminescence images," *Solar Energy*, vol. 185, pp. 455–468, 2019.

[10] B. Su, H. Chen, P. Chen, G. Bian, K. Liu, and W. Liu, "Deep learning-based solar-cell manufacturing defect detection with complementary attention network," *IEEE Transactions on Industrial Informatics*, vol. 17, no. 6, pp. 4084–4095, 2020.

[11] S. Ren, K. He, R. Girshick, and J. Sun, "Faster r-cnn: Towards real-time object detection with region proposal networks," *Advances in neural information processing systems*, vol. 28, 2015.

[12] M. W. Akram, G. Li, Y. Jin, X. Chen, C. Zhu, X. Zhao, A. Khaliq, M. Faheem, and A. Ahmad, "Cnn based automatic detection of photovoltaic cell defects in electroluminescence images," *Energy*, vol. 189, p. 116319, 2019.

[13] H. Liu, W. Ding, Q. Huang, and L. Fang, "Research on online defect detection method of solar cell component based on lightweight convolutional neural network," *International Journal of Photoenergy*, vol. 2021, pp. 1–13, 2021.

[14] L. Pratt, D. Govender, and R. Klein, "Defect detection and quantification in electroluminescence images of solar pv modules using u-net semantic segmentation," *Renewable Energy*, vol. 178, pp. 1211–1222, 2021.

[15] W. Tang, Q. Yang, X. Hu, and W. Yan, "Deep learning-based linear defects detection system for large-scale photovoltaic plants based on an edge-cloud computing infrastructure," *Solar Energy*, vol. 231, pp. 527–535, 2022.

[16] U. Otamendi, I. Martinez, M. Quartulli, I. G. Olaizola, E. Viles, and W. Cambarau, "Segmentation of cell-level anomalies in electroluminescence images of photovoltaic modules," *Solar Energy*, vol. 220, pp. 914–926, 2021.

[17] J. J. Vega Díaz, M. Vlaminck, D. Lefkaditis, S. A. Orjuela Vargas, and H. Luong, "Solar panel detection within complex backgrounds using thermal images acquired by uavs," *Sensors*, vol. 20, no. 21, p. 6219, 2020.

[18] N. Otsu, "A threshold selection method from gray-level histograms," *IEEE transactions on systems, man, and cybernetics*, vol. 9, no. 1, pp. 62–66, 1979.

[19] S. Suzuki *et al.*, "Topological structural analysis of digitized binary images by border following," *Computer vision, graphics, and image processing*, vol. 30, no. 1, pp. 32–46, 1985.

[20] A. Paszke, A. Chaurasia, S. Kim, and E. Culurciello, "Enet: A deep neural network architecture for real-time semantic segmentation," *arXiv preprint arXiv:1606.02147*, 2016.

[21] J. Yu, Y. Jiang, Z. Wang, Z. Cao, and T. Huang, "Unitbox: An advanced object detection network," in *Proceedings of the 24th ACM international conference on Multimedia*, pp. 516–520, 2016.

[22] R. O. Duda and P. E. Hart, "Use of the hough transformation to detect lines and curves in pictures," *Communications of the ACM*, vol. 15, no. 1, pp. 11–15, 1972.